

Frequency-Dependent Relationship Between Resting-State Functional Magnetic Resonance Imaging Signal Power and Head Motion Is Localized Within Distributed Association Networks

Jieun Kim,¹ Koene R.A. Van Dijk,^{1,2} Alexandra Libby,¹ and Vitaly Napadow¹

Abstract

Recent studies have highlighted the importance of analyzing spectral power in resting-state functional magnetic resonance imaging (rs-fMRI) data. Significant modulation of power has been ascribed to the performance of cognitive tasks and has been ascribed clinical significance. However, the role of confounding factors such as head motion on spectral power is not fully understood. Specifically, the spatial distribution of frequency-dependent associations between rs-fMRI power and motion is unknown. We utilized a large rs-fMRI dataset ($n=1000$) to quantify the influence of head motion on spectral power in different frequency bands. We (1) performed regression analyses across the entire sample and (2) computed difference maps between high- and low-motion groups, more consistent with common experimental designs, and both analyses gave similar results. Greater head motion led to reduced spectral power at lower frequencies (0.007–0.05 Hz), but increased power at higher frequencies (0.12–0.167 Hz). Importantly, our whole-brain voxel-wise analysis showed that brain areas in distributed association networks (e.g., default mode and frontoparietal control networks) were most susceptible to head motion. These results were consistent with or without global signal regression (GSR). Additionally, without GSR, we noted a positive correlation with low-frequency power in the pre- and postcentral gyrus (S1/M1), mid-cingulate cortex, and insula and a negative correlation with mid-frequency (0.05–0.12 Hz) power in S1/M1, visual, and lateral temporal cortices. Hence, head motion significantly affects rs-fMRI power and great care must be taken when assigning a diagnostic marker for clinical populations known to present with greater head motion.

Key words: head motion; resting-state functional MRI (rs-fMRI); spectral power

Introduction

CONNECTIVITY ANALYSES OF resting-state functional magnetic resonance imaging (rs-fMRI) data have been widely used to evaluate communication within and between different brain networks. While the most common approaches to rs-fMRI data analysis include seed-based correlation analysis and independent component analysis (ICA), spectral power analysis of rs-fMRI data has been growing more popular. This approach explores the strength of spontaneous fMRI data fluctuations within different frequency bands. Multiple studies have reported significant differences in rs-fMRI spectral power compared with similar data acquired during the performance of a cognitive or attention demanding task

(Baria et al., 2011; Dong et al., 2012; Duff et al., 2008; Salvador et al., 2008). In addition, group-level differences in spectral power have been shown for a number of neurologic and psychiatric disease states, including depression (Wang et al., 2012), schizophrenia (Yu et al., 2012), chronic pain disorder (Baliki et al., 2011; Malinen et al., 2010), Alzheimer's disease (Wang et al., 2011; Xi et al., 2012), and post-traumatic stress disorder (Bing et al., 2013). However, the origin of rs-fMRI spectral power at different frequencies is not well understood, and the influence of pernicious confounds such as head motion, which commonly differs between control and clinical populations, is also unknown.

Recently, several studies have highlighted the effects of in-scanner head motion on functional connectivity MRI outcome

¹Department of Radiology, MGH/MIT/HMS Athinoula A. Martinos Center for Biomedical Imaging, Massachusetts General Hospital, Charlestown, Massachusetts.

²Department of Psychology, Center for Brain Science, Harvard University, Cambridge, Massachusetts.

measures (Power et al., 2012; Satterthwaite et al., 2012, 2013; Van Dijk et al., 2012). For instance, Van Dijk and colleagues (2012) found that greater head motion was associated with decreased functional correlation strength among regions within the default mode network (DMN) and the frontoparietal control network (FPCN). Moreover, Power and associates (2012) found that subject movement decreased long-distance correlation strength and increased short-distance correlation strength in rs-fMRI data. Satterthwaite and associates found both correlative (Satterthwaite et al., 2012) and group difference (Satterthwaite et al., 2013) associations between head motion and frequency-specific spectral power over an averaged whole-brain sampling space. However, despite the growing interest of spectral power analysis for rs-fMRI data, the spatial distribution of the frequency-dependent association between rs-fMRI signal power and head motion is currently unknown.

In this study, we utilized a large rs-fMRI dataset ($n=1000$) to quantify the influence of head motion on spectral power in different frequency bands. We performed linear regression analyses and computed difference maps, consistent with common experimental designs for evaluating different clinical populations. We hypothesized that the rs-fMRI signal within distributed association networks would demonstrate a significant influence of head motion on the spectral power within specific frequency bands.

Methods

Subjects

rs-fMRI data were collected from $n=1000$ healthy young adults (57% women, age = 20.6 ± 2.4 years; mean \pm SD) without a history of neurological or psychiatric disorders. fMRI data were not included if scanner-induced artifacts were detected or if there was a low temporal signal-to-noise ratio. This dataset has been characterized in a previous publication (Van Dijk et al., 2012).

Imaging data acquisition

All data were collected on matched 3T Tim Trio scanners (Siemens, Erlangen, Germany) located at Harvard University and the Martinos Center for Biomedical Imaging, Massachusetts General Hospital, using a 12-channel phased-array head coil. The functional imaging data consisted of a single run of an echo-planar imaging (EPI) sequence sensitive to the blood oxygenation level-dependent (BOLD) signal (TR/TE = 3000/30 ms, flip angle = 85° , $3 \times 3 \times 3$ mm³, 47 AC-PC aligned axial slices, 124 volumes). Structural data included a high-resolution multiecho T1-weighted magnetization-prepared gradient-echo sequence. Foam pillows and extendable padded head clamps were used to limit head motion. During the scan, subjects were instructed to rest in the scanner with their eyes open, while staying as still as possible.

Resting-State fMRI Data Analysis Overview

First, a linear regression analysis was performed that utilized the entire sample ($N=1000$). Second, subjects were divided into ten groups based on their mean motion during the run. The group of 100 subjects who moved the least was compared with the group of 100 subjects who moved the most. Men tend to move more than women (Van Dijk

et al., 2012), and the gender distribution between the two groups was not equal. To control for these gender differences, 17 women in the low-motion group were replaced with a random sampling of 17 men from the penultimate least motion group. Similarly, five men from the high-motion group were replaced with a random sampling of five women from the penultimate high-motion group. Following this procedure, the two subsample groups of 100 subjects each were not significantly different with respect to either age or gender (Low motion: 50% women, 21.1 ± 1.9 years; High motion: 50% women, 21.2 ± 2.6 years).

Functional MRI data preprocessing

Functional MRI data were processed using the validated FSL (FMRIB's Software Library, www.fmrib.ox.ac.uk/fsl/) and SPM2 (www.fil.ion.ucl.ac.uk/spm/) software packages. The first four volumes of each run were discarded to allow for T1-equilibration effects. Typical rs-fMRI data preprocessing analyses were performed. This included slice timing correction and affine head motion correction (Jenkinson et al., 2002). Atlas registration was achieved by computing affine transforms that coregister the first volume of the functional data using SPM2 with a BOLD EPI template in the Montreal Neurological Institute (MNI) space (Evans et al., 1993). Data were resampled to 2-mm isotropic voxels and spatially smoothed using a 6-mm full-width half-maximum (FWHM) Gaussian kernel. High-pass filtering was applied to remove constant offsets while retaining frequencies above 0.007 Hz. Several sources of spurious or regionally nonspecific variance were removed by regression of nuisance variables that include (1) the six translation and rotation parameters of the rigid body head motion correction step [also high-pass filtered above 0.007 Hz, as suggested by (Hallquist et al., 2013)], as well as time-series signals averaged over (2) the lateral ventricles, and (3) regions centered in the deep cerebral white matter (Fox et al., 2006; Van Dijk et al., 2010; Vincent et al., 2008). The lateral ventricles and white matter masks were applied in MNI space to the BOLD EPI data of each individual subject after these data were transformed to MNI space. Since global signal regression (GSR) is a controversial preprocessing step for rs-fMRI data (Fox et al., 2009; Murphy et al., 2009; Saad et al., 2012), we evaluated the effects of head motion on spectral power both "without GSR" and "with GSR." Regression of each of these signals was performed simultaneously using a general linear model, and the residual volumes were used for the spectral power analysis.

Head motion definition

Head motion was computed using the same methods as previously reported by Van Dijk and colleagues (2012) and based on the translational parameters in the x (left/right), y (anterior/posterior), and z (superior/inferior) directions obtained from the rigid body motion correction step. Our motion metric was based solely on estimated translational head motion. While the linear correlation between estimated translation and rotation was high [$r=0.96$, Van Dijk et al. (2012)], assessment of possible difference between translation-based metric and full translation plus rotation-based metric is beyond the scope of the present article. Displacement in 3D space for each brain volume was computed as the root-mean-square of the translation parameters and expressed in mm.

Mean relative motion represents the mean displacement in 3D space of each brain volume as compared with the previous volume (volume-based relative displacement = $\sqrt{x_t^2 + y_t^2 + z_t^2} - \sqrt{x_{t-1}^2 + y_{t-1}^2 + z_{t-1}^2}$).

Spectral power analysis

Spectral analysis was performed on the 4D BOLD residual signal using 3dPeriodogram (AFNI, <http://afni.nimh.nih.gov/afni/>). For each subject, the frequency power of the BOLD signal was determined for each voxel and normalized by dividing by total power. Three frequency bands were defined: low frequency, 0.007–0.05 Hz; mid frequency, 0.05–0.12 Hz; and high frequency, 0.12–0.167 Hz, as in previous studies (Baliki et al., 2011; Malinen et al., 2010). The average spectral power of each frequency band was calculated at each voxel.

To evaluate spectral characterization of the global signal, we performed Fourier transformation (1dFFT-AFNI) on the averaged signal over a whole-brain mask for each individual subject. Spectral power and proportion of power to total power were computed in each of the frequency bands.

Group analyses

Individuals' MNI-space spectral power maps were then passed up to group-level analyses performed using a mixed-effects model (FEAT, FSL). To evaluate the correlation between each spectral power map and mean head motion, we performed a linear regression with individuals' spectral power maps as the dependent variable. Age and gender were used as regressors of no interest in the regression model. In an additional analysis, subjects were separated into an $n = 100$ high-motion group and an $n = 100$ low-motion group. This analysis was meant to approximate common two-group comparison analyses, such as between patients and controls, wherein one group moves significantly more than the other. Statistical difference maps between the low- and high-motion subgroups were computed using an unpaired two-sample t -test. This was done for each of the three spectral power bands. Since previous results indicate that the relationship between head motion and two large-scale association networks was better modeled by a linear regression than by a nonlinear regression (Van Dijk et al., 2012), we wanted to test whether adding head motion as regressor of no interest in the across-group analysis might mitigate any differences in spectral power between the two groups. Thus, we repeated the analysis adding the de-meaned head motion score as a regressor of no interest. Age was used as a nuisance regressor in both analyses (we should note that not including age as a nuisance regressor in the model resulted in identical brain areas that pass our statistical threshold, data not shown). Brain maps were thresholded using cluster correction for multiple comparisons with a cluster-forming threshold of $Z > 2.3$ and a cluster-size threshold of $p < 0.01$. All corrected maps were projected to a surface display using `mri_vol2surf` (`surfer.nmr.mgh.harvard.edu`).

To quantify the spatial specificity of the association between head motion and spectral power of the rs-fMRI signal, we calculated the number of significant voxels within masks of previously defined canonical functional brain networks as made available by Yeo and colleagues (2011). Yeo and associates (2011) defined sensory and motor cortices (visual and somatomotor network, referred to as Visual and SMN, re-

spectively) as well as large distributed networks of association cortex including those referred to as the dorsal and ventral attention network [DAN and VAN, respectively (Fox et al., 2006)], the FPCN (Dosenbach et al., 2007; Vincent et al., 2008), and the DMN (Buckner et al., 2008; Greicius et al., 2003; Raichle et al., 2001). Labels for these networks are used in the present article as a heuristic and are generally similar to functional parcellations of the brain when other methods are used [e.g., seed based and ICA (Beckmann et al., 2005; Vincent et al., 2008)]. Regions of a "limbic network" (Limbic) cover areas of the temporal and orbitofrontal cortex and may contain both neuronal and noise signals, as these regions are near areas known to be affected by MR susceptibility artifacts (Yeo et al., 2011).

Results

A whole-brain linear regression analysis evaluated the influence of head motion on spectral power in low- (0.007–0.05 Hz), mid- (0.05–0.12 Hz), and high-frequency (0.12–0.167 Hz) bands for rs-fMRI data. Without GSR, head motion was positively correlated with low-frequency power in the pre- and postcentral gyrus (S1/M1), mid-cingulate cortex (MCC), and insula that, according to maps published by Yeo and associates (2011), primarily fall in the SMN and VAN (see Fig. 1 and Supplementary Table S1; Supplementary Data are available online at www.liebertpub.com/brain). In addition, without GSR, head motion was negatively correlated with low-frequency power in medial prefrontal cortex (MPFC) and lateral temporal cortex (LTC). With GSR, a negative correlation between head motion and spectral power was found for the low-frequency band in MPFC, posterior cingulate cortex (PCC), precuneus (pCun), LTC, hippocampal formation (HF), inferior parietal lobule (IPL, i.e., DMN) and dorsolateral prefrontal (dlPFC, i.e., FPCN), and mid-cingulate cortices (see Fig. 1 and Supplementary Table S2).

Without GSR, head motion was negatively correlated with mid-frequency band power in S1/M1 and visual and lateral cortices, while with GSR, there were no regions that show a significant association between head motion and spectral power in mid-frequency band. In addition, our analysis showed a positive correlation between head motion and spectral power in the high-frequency band in the MPFC, PCC, pCun, LTC, IPL (i.e., DMN), and dlPFC (i.e., FPCN), regardless of whether GSR was used or not (see Fig. 1 and Supplementary Tables S1 and S2). We further quantified the spatial specificity of the association between head motion and spectral power of the rs-fMRI signal, by calculating the number of significant voxels within masks of canonical functional brain networks based on Yeo and associates (2011). GSR influenced the spatial distribution of the relationship between head motion and spectral power in lower, but not higher, frequencies. We found that the association between greater head motion and greater high-frequency power was primarily located in the large distributed networks of association cortex, mostly in the DMN and FPCN (see the last column in Fig. 1). To illustrate the distribution of these effects in this sample of 1000 subjects, we plotted the association between mean motion and low-frequency and high-frequency power as extracted from the earlier-mentioned MPFC regions (see Fig. 2).

For separate analyses, a low-motion group and a high-motion group were selected based on the mean head motion

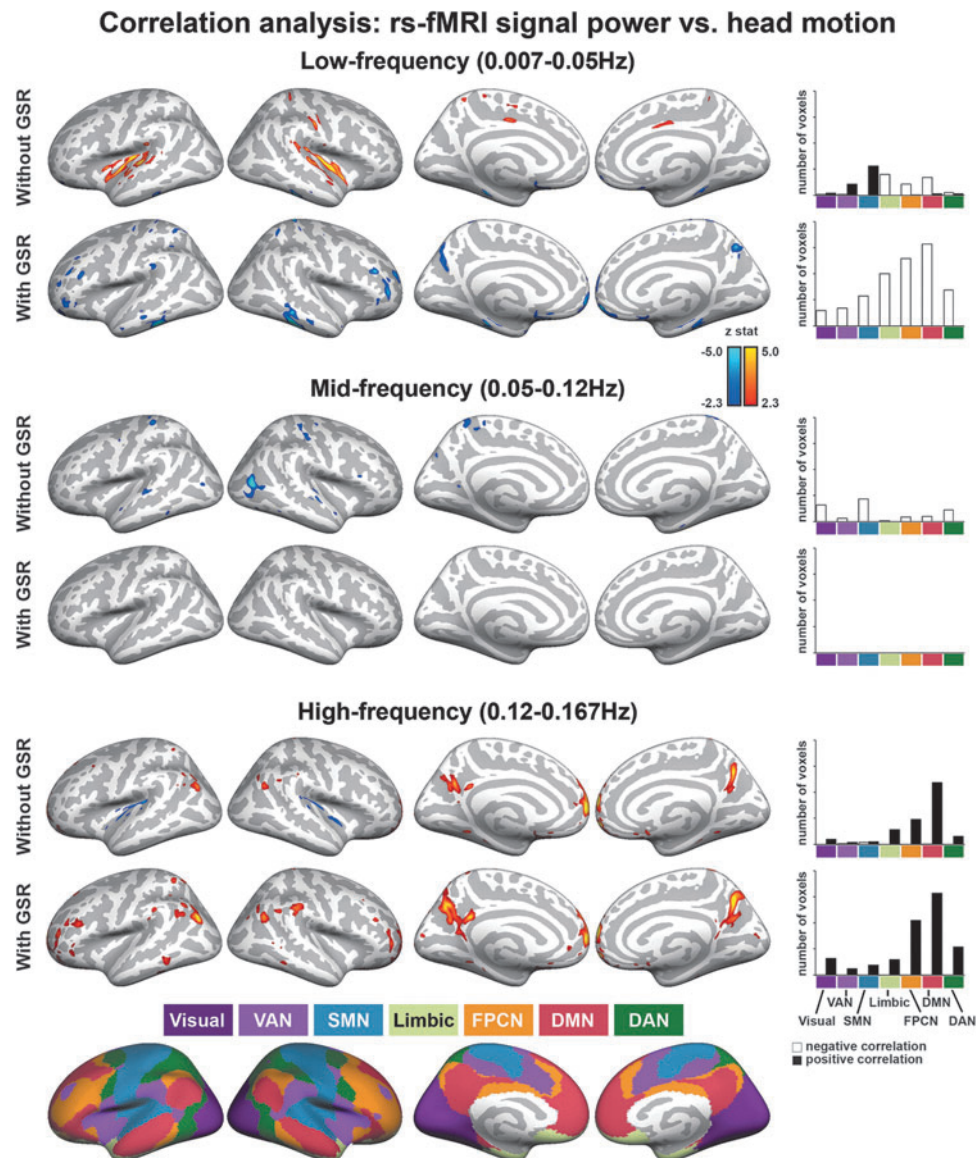


FIG. 1. Frequency- and region-dependent correlations between head motion and rs-fMRI spectral power across all subjects ($n=1000$). Without GSR, greater head motion during rs-fMRI scanning was associated with lesser low-frequency power in MPFC and LTC (i.e., DMN) and greater low-frequency power in the pre- and postcentral gyrus (i.e., SMN), mid-cingulate cortex and insula (i.e., VAN); lesser mid-frequency power in the SMN and visual network; and greater high-frequency power in DMN and FPCN. With GSR, brain regions in DMN and FPCN similarly exhibited lesser low-frequency power and greater high-frequency power in subjects with greater head motion. Bar plots in the right column represent the network allocations and the number of voxels show significant correlations with head motion. White bars denote the number of voxels showing a negative correlation with head motion, while black bars denote the number of voxels showing a positive correlation with head motion [y axes of the bar plots scale from 0 to 8000 with a 2000 tick; Visual, visual network; GSR, global signal regression; rs-fMRI, resting-state functional magnetic resonance imaging; VAN, ventral attention network; SMN, somatomotor network; Limbic, limbic network; FPCN, frontoparietal control network; DMN, default mode network; and DAN, dorsal attention network; Network masks as provided by Yeo et al. (2011)].

during the scan. The difference in relative mean head motion between the low- and high-motion groups was statistically significant (low motion: 0.019 ± 0.002 mm; high motion: 0.082 ± 0.023 , $t(198)=28.51$, $p < 0.001$). Results were consistent with the correlation analyses. For the low-frequency band, the high-motion group showed greater power than the low-motion group in the insula, and lower power in MPFC and

LTC (i.e., DMN), when GSR was not used. With GSR, we found that the high-motion group, compared with the low-motion group, showed lower low-frequency power in the MPFC, PCC, pCun, LTC, IPL (i.e., DMN), and dIPFC (i.e., FPCN). For the high-frequency band, the high-motion group demonstrated significantly greater spectral power in MPFC, PCC, pCun, LTC, IPL (i.e., DMN), and dIPFC

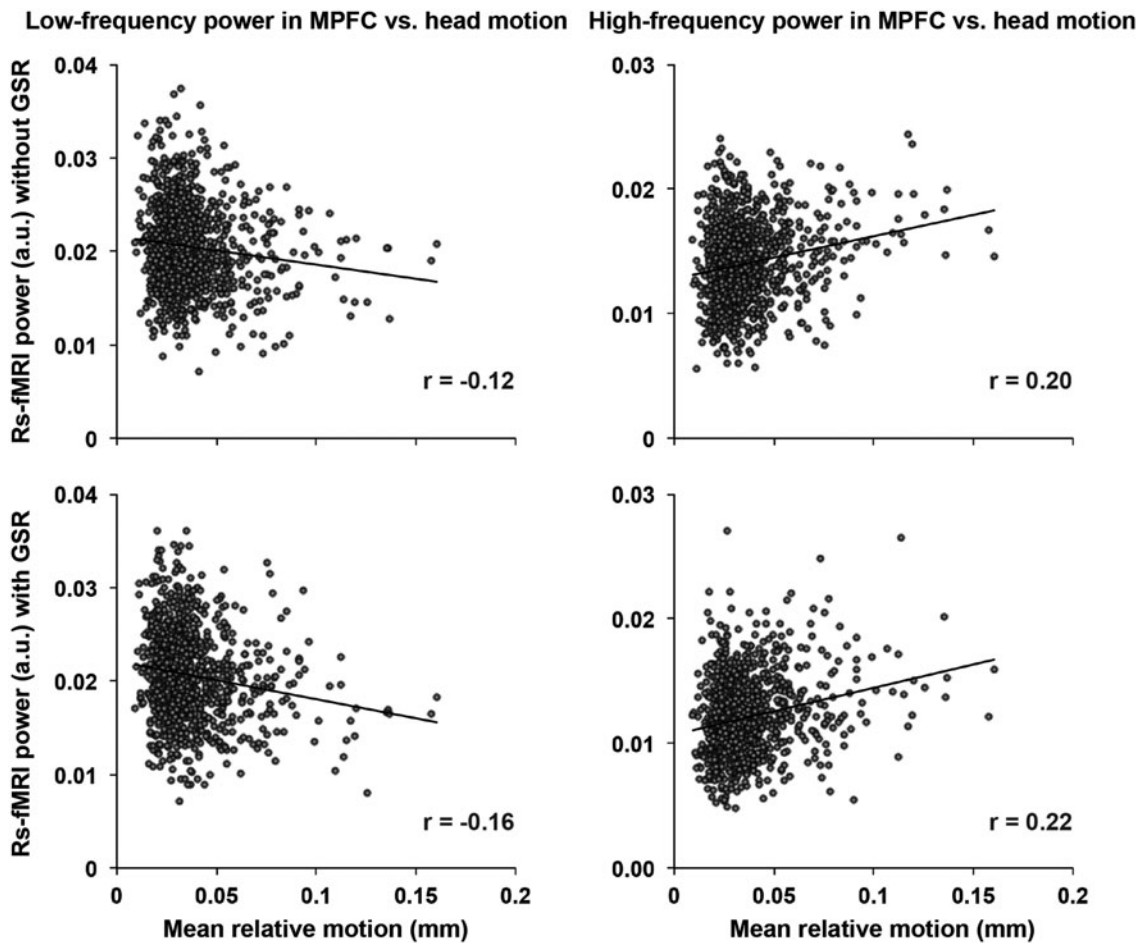


FIG. 2. Head motion correlation with rs-fMRI spectral power in MPFC. Head motion shows a significant negative correlation with spectral power in the low-frequency band (left) and a positive correlation with spectral power in the high-frequency band (right) in the MPFC. The relationship was significant with or without GSR. Each dot represents a single subject. MPFC, medial prefrontal cortex.

(i.e., FPCN), without regard to whether GSR was used or not (see Fig. 3, and Supplementary Tables S3 and S4). For the mid-frequency band, the high-motion group showed lower power than the low-motion group in S1/M1 and visual and lateral cortices, only when GSR was not applied.

An averaged spectral power plot from the low-frequency and high-frequency bands for both the MPFC and PCC clearly demonstrated that the high-motion group showed less power at low frequencies and greater power at high frequencies, with no significant differences at mid frequencies (see Fig. 4).

These results corroborate the results of the linear regression analysis that were based on the full sample, but more clearly demonstrate the effects of motion on both the high- and low-frequency rs-fMRI signal power using an analysis approach that is often applied in studies that investigate differences in resting-state functional connectivity patterns between a patient population and a control group or between groups with different ages.

Because our previous study indicated that the relationship between head motion and two large-scale association networks was better modeled by a linear regression than by a nonlinear regression (Van Dijk et al., 2012), we wanted to

test whether adding head motion as regressor of no interest in the between-group analysis (based on linear statistical modeling) might mitigate possible effects of motion on spectral power. Therefore, we repeated the two-group voxel-wise contrast analysis with mean motion included as a regressor of no interest. Results showed that nearly all of the spectral power differences between low- and high-motion groups disappeared. Without GSR, the 613 voxel MPFC cluster that showed lower low-frequency power in the high-motion group disappeared completely when mean motion was included as regressor of no interest. With GSR, the 1298 voxel MPFC cluster that similarly showed lower low-frequency power in the high-motion group was reduced to only 24 voxels. For the mid- and high-frequency power bands, addition of mean motion as regressor of no interest eliminated any significant influence of motion on rs-fMRI signal power.

Our results showed that GSR influenced the relationships between head motion and spectral power for lower, but not higher, frequencies. To better understand why this was the case, we characterized the power spectrum of the global signal. The global signal power spectrum showed a greater proportion of low-frequency power and lower proportion of high-frequency power, when compared to a brain area such

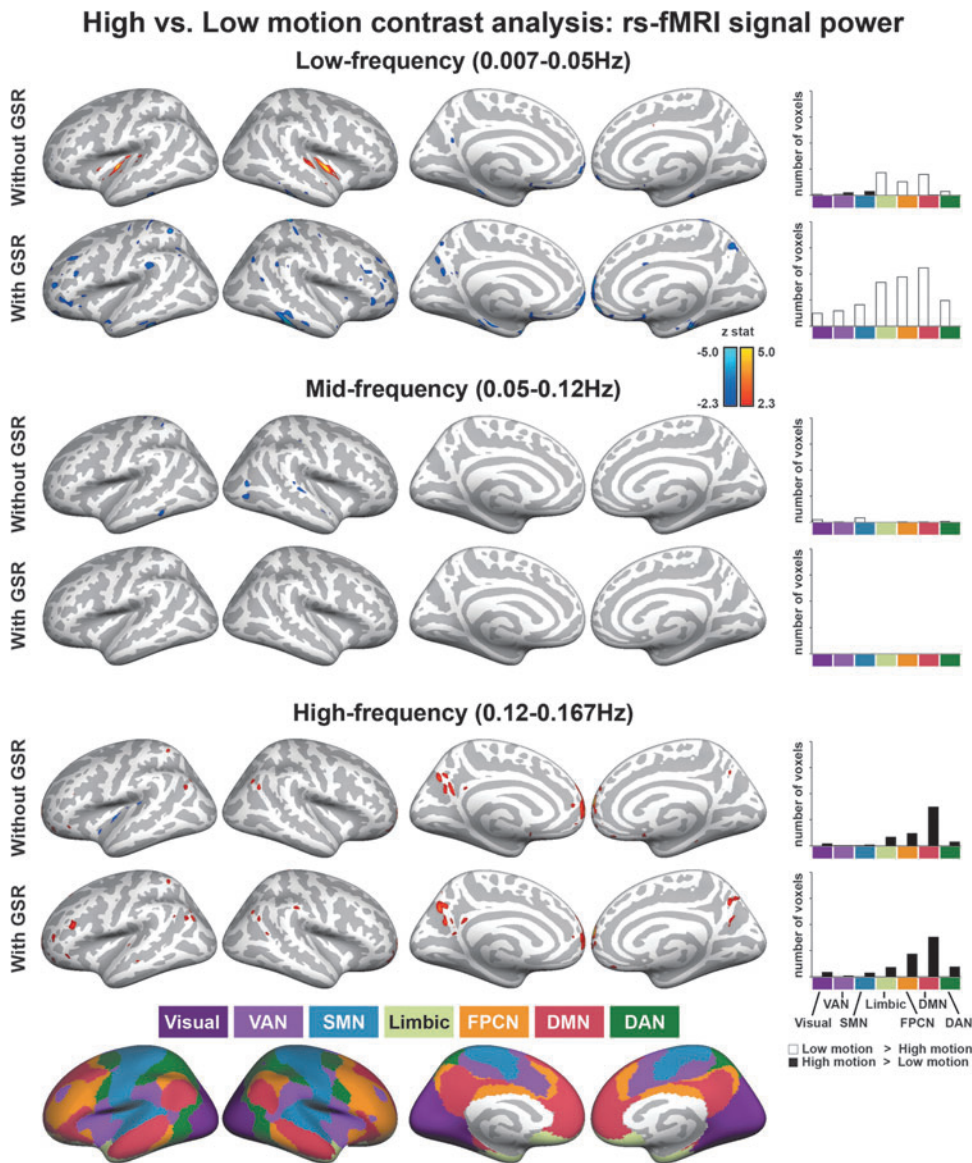


FIG. 3. Frequency dependence of spectral power difference maps between high-motion ($n=100$) and low-motion ($n=100$) groups. Without GSR, compared with the low-motion group, the high-motion group demonstrated less low-frequency power in the MPFC and LTC (i.e., DMN regions) and greater low-frequency power in the insula. High-motion group subjects also demonstrated less mid-frequency power in visual and lateral cortices. With GSR, subjects with greater head motion showed less low-frequency power in MPFC, PCC, LTC, IPL (i.e., DMN), and dIPFC (i.e., FPCN). High-motion group subjects also showed greater high-frequency spectral power in MPFC, PCC, LTC, and IPL (i.e., DMN) and dIPFC (i.e., FPCN) areas, regardless of whether GSR was used or not (y axes of the bar plots in the most right column scale from 0 to 8000 with a 2000 tick). LTC, lateral temporal cortex; PCC, posterior cingulate cortex; IPL, inferior parietal lobule.

as the MPFC, where head motion was associated with high-frequency power (e.g., low-frequency band: global signal=88%, MPFC=81%, $t(999)=42.12$, $p<0.001$; high-frequency band: global signal=11%, MPFC=19%, $t(999)=-42.12$, $p<0.001$). This might explain why GSR particularly influenced low-frequency band results.

Discussion

Our results demonstrate that head motion significantly influences spectral power estimates in rs-fMRI data even when motion correction and additional voxel-wise regression of the motion correction parameters on the single-subject level is utilized. Our whole-brain analysis showed that increased in-scanner head motion is associated with increased high-frequency power in large distributed association networks, primarily in the DMN and FPCN regardless of whether GSR was used or not. While some relationships between head motion and power at lower frequencies were altered by GSR, motion-related reduction of low-frequency power

in the DMN remained consistent. When we did not apply GSR, we found that some brain regions showed increased power with increased motion and other regions showed decreased power with increasing motion in the low-frequency band. When GSR was applied, all effects were negative; that is, throughout different networks, higher motion was associated with lesser power. We speculate that GSR shifted the distribution of motion-spectral power associations, consistent with the well-known shift in the distribution of inter-regional correlation values in typical rs-fMRI connectivity analyses. Future studies should address GSR's influence on the linkage between power and connectivity outcomes in rs-fMRI analysis.

These results were found using both a linear regression analysis approach and also when performing a two-group comparison. The latter is more typically applied by investigators who want to investigate neuronal differences between a patient population and a control group or between groups of different ages. Importantly, when mean head motion across the run was included in our group comparison approach, the spectral power differences in the location where they

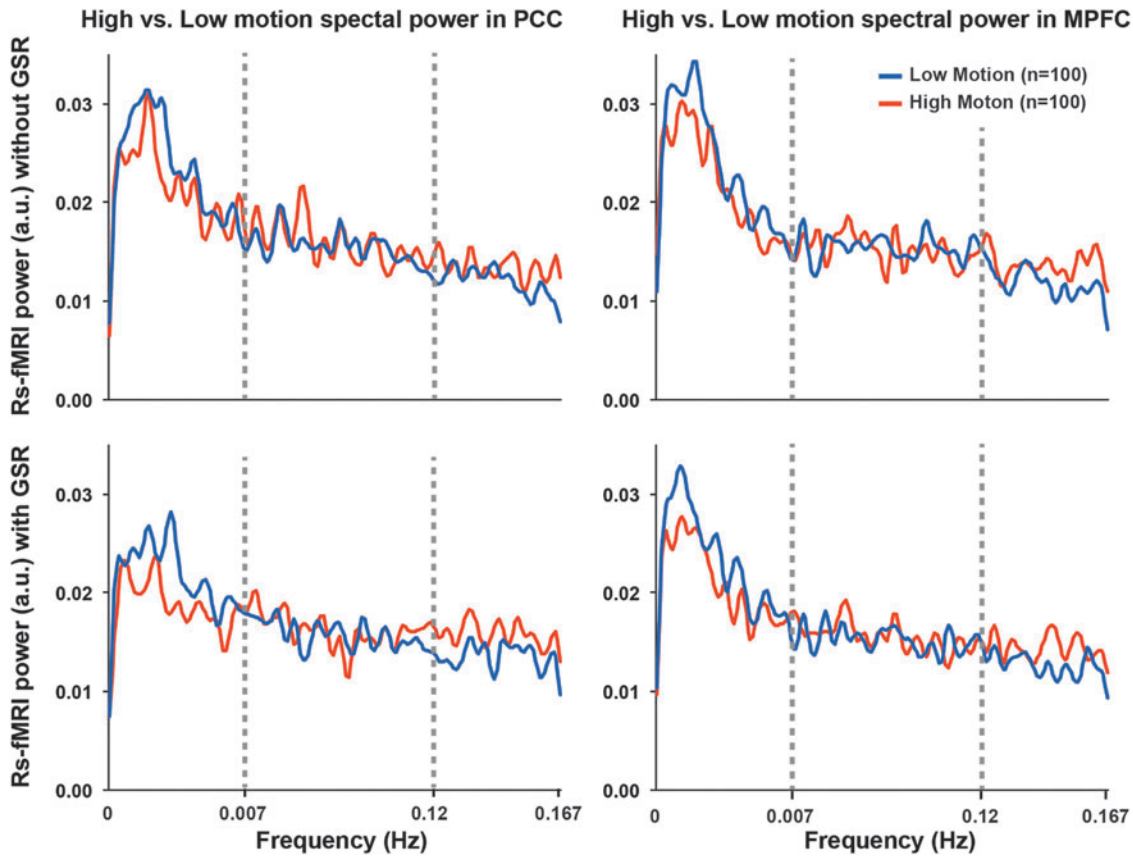


FIG. 4. rs-fMRI spectral power differs between high and low head motion groups. Row 1 shows the magnitude power spectra for the fMRI timeseries taken from the PCC (left) and MPFC (right) without GSR. Row 2 shows the magnitude spectra from the PCC and MPFC with GSR. The high-motion group showed less power at low frequencies (LF: 0.007–0.05 Hz) and greater power at high frequencies (HF: 0.12–0.167 Hz) in both PCC and MPFC. No significant differences were found at mid frequencies (MF: 0.05–0.12 Hz).

were most prominent either lost their significance (e.g., high-frequency band and low-frequency band without GSR) or diminished drastically (e.g., low-frequency band with GSR). This finding supports the contention that head motion explains a small but significant portion of the variance in high- and low-frequency spectral power in rs-fMRI data.

Because rs-fMRI signal power is maximal at low frequencies (<0.1 Hz) (Beckmann et al., 2005; Cordes et al., 2001; Kiviniemi et al., 2003), many previous rs-fMRI power analysis studies have focused on the low-frequency oscillation band. For instance, previous studies have characterized the amplitude of low-frequency fluctuations (ALFFs) that occur between 0.01 and 0.08 Hz (Zou et al., 2008). Further, patients have been reported to show both greater and lesser power in a low-frequency band (Bing et al., 2013; Liu et al., 2012; Wang et al., 2011; Xi et al., 2012; Yu et al., 2012), without specifically testing for the influence of head motion on these group differences. Hlinka and colleagues reported that head motion positively correlates with ALFF in ROIs containing motor, visual, auditory, and default mode networks during sedation in a relatively small sample (i.e., ALFF was positively correlated with head motion; $n=20$) (Hlinka et al., 2010). In contrast, other studies that use data from a larger number of healthy young participants (Satterthwaite et al.: $n=421$, Yan et al.: $n=158$) found a negative correlation between head motion and fALFF (ratio of low-frequency fluctu-

ations to the entire spectrum) throughout the cortex (Satterthwaite et al., 2012; Yan et al., 2013). However, in a separate ROI-based analysis with $n=200$ healthy young adults, Satterthwaite and colleagues also reported that subjects with greater head motion had *greater* power at low frequencies (Satterthwaite et al., 2013), thus supporting the results of Hlinka and associates. Our results with $n=1000$ subjects suggest that greater head motion is associated with lesser low-frequency power and that large distributed association networks, primarily the DMN and FPCN, are most acutely affected by this phenomenon. The incongruity for the low-frequency spectrum evident in currently available data may have been due to differences in sample sizes and/or averaging spectral power metrics from multiple unrelated brain networks/regions. Nevertheless, our data show that head motion does influence low-frequency power of rs-fMRI data.

A few rs-fMRI power studies have also investigated the higher frequency oscillation band (Baliki et al., 2011; Baria et al., 2011; Cauda et al., 2009; Malinen et al., 2010), though slight differences are noted in what constitutes “high-frequency” in these studies: Malinen and associates (2010), 0.12–0.25 Hz; Baliki and colleagues (2011), 0.12–0.2 Hz; Baria and colleagues (2011), 0.15–0.2 Hz; and Cauda and associates (2009), 0.1–0.25 Hz. In these studies, the influence of head motion was not specifically addressed, and group differences in high-frequency spectral power were

attributed to the pathophysiology of a disease process (i.e., chronic pain) or complex information processing for a given task. Additionally, Salvador and colleagues reported that a mutual information coherence metric was significantly influenced by head motion at higher frequencies compared with lower frequencies, further supporting the contention that estimates of connectivity at higher frequencies may be more susceptible to head motion artifacts (Salvador et al., 2008). In a more general composite analysis, Satterthwaite and associates reported that high head motion resulted in significantly greater high-frequency (0.08–0.16 Hz) power, as assessed from an averaged signal from 160 regions covering the entire brain (Satterthwaite et al., 2013). Our results support the contention that head motion is positively correlated with high-frequency power and that these effects are localized in large association networks.

Interestingly, most brain regions where rs-fMRI spectral power was affected by head motion are key nodes of the DMN (Buckner et al., 2008; Greicius et al., 2003; Raichle et al., 2001) and FPCN (Dosenbach et al., 2007; Vincent et al., 2008), particularly when GSR was used. While functional connectivity among DMN brain regions is high during both tasks and rest (Fransson, 2006; Smith et al., 2009; Van Dijk et al., 2010), the DMN is known to be more active when subjects are at rest and perhaps engaged in internally oriented thought and self-referential mentation (Buckner et al., 2008; Gusnard et al., 2001). Diminished low-frequency power within the DMN during increased head motion may have resulted from the subject being uncomfortable in the scanner, which possibly results in subjects (1) moving more in an attempt to become more comfortable and (2) being less engaged in self-referential cognition during actuation of this in-scanner motion. The first possibility would limit the signal-to-noise ratio of the rs-fMRI data (and we know that mean head motion is significantly related to temporal signal-to-noise ratio of the data; Van Dijk et al., 2012), obscuring measurement of the true neuronal signal. The second possibility would reduce actual neuronal activity in DMN brain regions perhaps resulting in frequency-specific changes in rs-fMRI spectral power. While this latter point is speculative it is supported by findings that an externally focused visual-motor task has been shown to decrease low-frequency power and increase high-frequency power in DMN regions such as the MPFC (Baria et al., 2011). Future studies should explore whether increased head motion during performance of tasks that rely on DMN function contributes to shifting power profiles within specific power bands.

In rs-fMRI data, the DMN is typically characterized by slow oscillations, with peak power occurring at frequencies significantly lower than 0.1 Hz (i.e., within our defined low-frequency band). However, a recent study has suggested that within the DMN, high-frequency power can dominate in MPFC (specifically pregenual and subgenual anterior cingulate cortices) subregions, while lower frequencies may be dominant in a PCC subregion (Baria et al., 2011). In our analyses, the DMN was related to head motion in a more monolithic manner; that is, all DMN subregions demonstrated less low-frequency power and more high-frequency power with greater head motion.

The FPCN is a distributed cortical network that supports higher level cognitive processing [i.e., working memory and cognitive control (Vincent et al., 2008)]. Our results demon-

strate lesser low-frequency power and greater high-frequency power with greater head motion in FPCN regions (e.g., dlPFC). The dlPFC may have been sensitive to this effect due to its location near the lateral brain surface where there is high MRI signal contrast due to the parenchyma–fluid interface. Approaches for examining the impact of head motion across different brain regions have shown that the medial and lateral prefrontal cortices (e.g., dlPFC and MPFC) exhibit a larger amount of motion compared with other regions (Satterthwaite et al., 2013; Yan et al., 2013), suggesting the existence of regional specificity for the influence of head motion.

GSR is commonly employed in analyses of rs-fMRI data to remove physiological noise that is believed to be common to all brain regions but has also been shown to mathematically mandate that negative correlations will occur (Buckner et al., 2008; Fox et al., 2009; Murphy et al., 2009; Van Dijk et al., 2010; Vincent et al., 2006). Others designate GSR as a highly controversial step based on fMRI data simulations (Saad et al., 2012). With regard to rs-fMRI signal power, Yan and associates recently demonstrated that the head motion influence on the ratio of low-frequency power (0.01–0.1 Hz) to that of the entire frequency range (fALFF) was characterized by a positive correlation within S1/M1, MCC, and insula and a negative correlation within DMN areas and that these relationships were not strongly affected by GSR (Yan et al., 2013). Our results corroborate those results for low-frequency power correlations with head motion, particularly when GSR was not applied.

We also found that GSR more strongly affected our results in low- and mid-band frequencies, both for the correlation analysis and two-group comparison. This was likely due to the fact that the power spectrum for the global signal (extracted signal from a whole-brain mask) was characterized by a greater proportion of lower frequency power compared to specific brain areas in which high-frequency power was associated with head motion (i.e., MPFC). While the origin of spectral power in the resting BOLD signal is not fully understood, head motion should be factored into spectral power analysis when considering areas that are part of the DMN and FPCN, which we found to be significantly susceptible to head motion.

It should be noted that head motion significantly correlated with spectral power even with standard motion correction and including motion corrected timeseries as nuisance regressor in the single-subject GLM. One possibility is that head motion nonlinearly affects the BOLD signal, and thus it is not easily removed with linear correction strategies. Future studies should investigate nonlinear relationships between head motion and the resting BOLD signal. Additionally, the lateral ventricle nuisance regressor mask was applied in MNI space on each individual's BOLD data, after these data were transformed to MNI space and spatially smoothed using a 6-mm FWHM Gaussian kernel. While this approach represents standard preprocessing procedures, imperfect fitting of the mask in MNI space may have resulted in blurring of signal across tissue boundaries, including some subcortical structures (e.g., caudate nucleus). While our aims were to investigate the influence of head motion on spectral power using standard preprocessing procedures, future studies should investigate the sensitivity of our results to different preprocessing strategies (e.g., Satterthwaite et al., 2013). Thus our findings warrant further research and also stress the need

for strict data-acquisition protocols (including clear and repeated instructions to study participants) and stringent data quality control.

Conclusion

Head motion significantly influences spectral power estimates in rs-fMRI data, and can confound group comparison even when motion correction by means of realignment of acquired brain volumes and voxel-wise regression of the motion correction parameters on the single-subject level is utilized. Our whole-brain voxel-wise analysis showed that large distributed association networks, primarily the default mode network and frontoparietal control network, appear to be susceptible to spectral power differences resulting from head motion. In these regions, increased head motion was associated with increased high-frequency power and diminished low-frequency spectral power. Our results extend previous assessments of the influence of head motion on rs-fMRI data and suggest that great care needs to be taken in assessing spectral power parameters in rs-fMRI data, particularly when attempting to assign a diagnostic marker for clinical populations, that are known to present with greater head motion in the scanner.

Acknowledgments

The authors thank Dr. Randy L. Buckner for providing the rs-fMRI data that were collected for the Brain Genomics Superstruct Project. The authors acknowledge the financial support from the NIH [R01-AT004714, R01-AT004714-02S1, P01-AT002048, R21-DK097499, and R01-AT005280] and NCCR [P41RR14075 and S10RR021110].

Author Disclosure Statement

The authors have no competing financial conflicts of interest to declare.

References

- Baliki MN, Baria AT, Apkarian AV. 2011. The cortical rhythms of chronic back pain. *J Neurosci* 31:13981–13990.
- Baria AT, Baliki MN, Parrish T, Apkarian AV. 2011. Anatomical and functional assemblies of brain BOLD oscillations. *J Neurosci* 31:7910–7919.
- Beckmann CF, DeLuca M, Devlin JT, Smith SM. 2005. Investigations into resting-state connectivity using independent component analysis. *Philos Trans R Soc Lond B Biol Sci* 360:1001–1013.
- Bing X, Ming-Guo Q, Ye Z, Jing-Na Z, Min L, Han C, Yu Z, Jia-Jia Z, Jian W, Wei C, Han-Jian D, Shao-Xiang Z. 2013. Alterations in the cortical thickness and the amplitude of low-frequency fluctuation in patients with post-traumatic stress disorder. *Brain Res* 1490:225–232.
- Buckner RL, Andrews-Hanna JR, Schacter DL. 2008. The brain's default network: anatomy, function, and relevance to disease. *Ann N Y Acad Sci* 1124:1–38.
- Cauda F, Sacco K, Duca S, Cocito D, D'Agata F, Geminiani GC, Canavero S. 2009. Altered resting state in diabetic neuropathic pain. *PLoS One* 4:e4542.
- Cordes D, Haughton VM, Arfanakis K, Carew JD, Turski PA, Moritz CH, Quigley MA, Meyerand ME. 2001. Frequencies contributing to functional connectivity in the cerebral cortex in "resting-state" data. *AJNR Am J Neuroradiol* 22:1326–1333.
- Dong ZY, Liu DQ, Wang J, Qing Z, Zang ZX, Yan CG, Zang YF. 2012. Low-frequency fluctuation in continuous real-time feedback of finger force: a new paradigm for sustained attention. *Neurosci Bull* 28:456–467.
- Dosenbach NU, Fair DA, Miezin FM, Cohen AL, Wenger KK, Dosenbach RA, Fox MD, Snyder AZ, Vincent JL, Raichle ME, Schlaggar BL, Petersen SE. 2007. Distinct brain networks for adaptive and stable task control in humans. *Proc Natl Acad Sci U S A* 104:11073–11078.
- Duff EP, Johnston LA, Xiong J, Fox PT, Mareels I, Egan GF. 2008. The power of spectral density analysis for mapping endogenous BOLD signal fluctuations. *Hum Brain Mapp* 29:778–790.
- Evans AC, Collins DL, Mills SR, Brown ED, Kelly RL, Peters TM. 1993. (3D statistical neuroanatomical models from 305 MRI volumes). In *Proc. IEEE-Nuclear Science Symposium and Medical Imaging Conference*, pp. 1813–1817.
- Fox MD, Corbetta M, Snyder AZ, Vincent JL, Raichle ME. 2006. Spontaneous neuronal activity distinguishes human dorsal and ventral attention systems. *Proc Natl Acad Sci U S A* 103:10046–10051.
- Fox MD, Zhang D, Snyder AZ, Raichle ME. 2009. The global signal and observed anticorrelated resting state brain networks. *J Neurophysiol* 101:3270–3283.
- Fransson P. 2006. How default is the default mode of brain function? Further evidence from intrinsic BOLD signal fluctuations. *Neuropsychologia* 44:2836–2845.
- Greicius MD, Krasnow B, Reiss AL, Menon V. 2003. Functional connectivity in the resting brain: a network analysis of the default mode hypothesis. *Proc Natl Acad Sci U S A* 100:253–258.
- Gusnard DA, Akbudak E, Shulman GL, Raichle ME. 2001. Medial prefrontal cortex and self-referential mental activity: relation to a default mode of brain function. *Proc Natl Acad Sci U S A* 98:4259–4264.
- Hallquist MN, Hwang K, Luna B. 2013. The nuisance of nuisance regression: Spectral misspecification in a common approach to resting-state fMRI preprocessing reintroduces noise and obscures functional connectivity. *Neuroimage* 82:208–225.
- Hlinka J, Alexakis C, Hardman JG, Siddiqui Q, Auer DP. 2010. Is sedation-induced BOLD fMRI low-frequency fluctuation increase mediated by increased motion? *Magma* 23:367–374.
- Jenkinson M, Bannister P, Brady M, Smith S. 2002. Improved optimization for the robust and accurate linear registration and motion correction of brain images. *Neuroimage* 17:825–841.
- Kiviniemi V, Kantola JH, Jauhiainen J, Hyvarinen A, Tervonen O. 2003. Independent component analysis of nondeterministic fMRI signal sources. *Neuroimage* 19:253–260.
- Liu CH, Li F, Li SF, Wang YJ, Tie CL, Wu HY, Zhou Z, Zhang D, Dong J, Yang Z, Wang CY. 2012. Abnormal baseline brain activity in bipolar depression: a resting state functional magnetic resonance imaging study. *Psychiatry Res* 203:175–179.
- Malinen S, Vartiainen N, Hlushchuk Y, Koskinen M, Ramkumar P, Forss N, Kalso E, Hari R. 2010. Aberrant temporal and spatial brain activity during rest in patients with chronic pain. *Proc Natl Acad Sci U S A* 107:6493–6497.
- Murphy K, Birn RM, Handwerker DA, Jones TB, Bandettini PA. 2009. The impact of global signal regression on resting state correlations: are anti-correlated networks introduced? *Neuroimage* 44:893–905.
- Power JD, Barnes KA, Snyder AZ, Schlaggar BL, Petersen SE. 2012. Spurious but systematic correlations in functional connectivity MRI networks arise from subject motion. *Neuroimage* 59:2142–2154.

- Raichle ME, MacLeod AM, Snyder AZ, Powers WJ, Gusnard DA, Shulman GL. 2001. A default mode of brain function. *Proc Natl Acad Sci U S A* 98:676–682.
- Saad ZS, Gotts SJ, Murphy K, Chen G, Jo HJ, Martin A, Cox RW. 2012. Trouble at rest: how correlation patterns and group differences become distorted after global signal regression. *Brain Connect* 2:25–32.
- Salvador R, Martinez A, Pomarol-Clotet E, Gomar J, Vila F, Sarro S, Capdevila A, Bullmore E. 2008. A simple view of the brain through a frequency-specific functional connectivity measure. *Neuroimage* 39:279–289.
- Satterthwaite TD, Elliott MA, Gerraty RT, Ruparel K, Loughhead J, Calkins ME, Eickhoff SB, Hakonarson H, Gur RC, Gur RE, Wolf DH. 2013. An improved framework for confound regression and filtering for control of motion artifact in the preprocessing of resting-state functional connectivity data. *Neuroimage* 64:240–256.
- Satterthwaite TD, Wolf DH, Loughhead J, Ruparel K, Elliott MA, Hakonarson H, Gur RC, Gur RE. 2012. Impact of in-scanner head motion on multiple measures of functional connectivity: relevance for studies of neurodevelopment in youth. *Neuroimage* 60:623–632.
- Smith SM, Fox PT, Miller KL, Glahn DC, Fox PM, Mackay CE, Filippini N, Watkins KE, Toro R, Laird AR, Beckmann CF. 2009. Correspondence of the brain's functional architecture during activation and rest. *Proc Natl Acad Sci U S A* 106:13040–13045.
- Van Dijk KR, Hedden T, Venkataraman A, Evans KC, Lazar SW, Buckner RL. 2010. Intrinsic functional connectivity as a tool for human connectomics: theory, properties, and optimization. *J Neurophysiol* 103:297–321.
- Van Dijk KR, Sabuncu MR, Buckner RL. 2012. The influence of head motion on intrinsic functional connectivity MRI. *Neuroimage* 59:431–438.
- Vincent JL, Kahn I, Snyder AZ, Raichle ME, Buckner RL. 2008. Evidence for a frontoparietal control system revealed by intrinsic functional connectivity. *J Neurophysiol* 100:3328–3342.
- Vincent JL, Snyder AZ, Fox MD, Shannon BJ, Andrews JR, Raichle ME, Buckner RL. 2006. Coherent spontaneous activity identifies a hippocampal-parietal memory network. *J Neurophysiol* 96:3517–3531.
- Wang L, Dai W, Su Y, Wang G, Tan Y, Jin Z, Zeng Y, Yu X, Chen W, Wang X, Si T. 2012. Amplitude of low-frequency oscillations in first-episode, treatment-naive patients with major depressive disorder: a resting-state functional MRI study. *PLoS One* 7:e48658.
- Wang Z, Yan C, Zhao C, Qi Z, Zhou W, Lu J, He Y, Li K. 2011. Spatial patterns of intrinsic brain activity in mild cognitive impairment and Alzheimer's disease: a resting-state functional MRI study. *Hum Brain Mapp* 32:1720–1740.
- Xi Q, Zhao XH, Wang PJ, Guo QH, Yan CG, He Y. 2012. Functional MRI study of mild Alzheimer's disease using amplitude of low frequency fluctuation analysis. *Chin Med J (Engl)* 125:858–862.
- Yan CG, Cheung B, Kelly C, Colcombe S, Craddock RC, Di Martino A, Li Q, Zuo XN, Castellanos FX, Milham MP. 2013. A comprehensive assessment of regional variation in the impact of head micromovements on functional connectomics. *Neuroimage* 76:183–201.
- Yeo BT, Krienen FM, Sepulcre J, Sabuncu MR, Lashkari D, Hollinshead M, Roffman JL, Smoller JW, Zollei L, Polimeni JR, Fischl B, Liu H, Buckner RL. 2011. The organization of the human cerebral cortex estimated by intrinsic functional connectivity. *J Neurophysiol* 106:1125–1165.
- Yu R, Chien YL, Wang HL, Liu CM, Liu CC, Hwang TJ, Hsieh MH, Hwu HG, Tseng WY. 2012. Frequency-specific alternations in the amplitude of low-frequency fluctuations in schizophrenia. *Hum Brain Mapp*. [Epub ahead of print]; doi: 10.1002/hbm.22203.
- Zou QH, Zhu CZ, Yang Y, Zuo XN, Long XY, Cao QJ, Wang YF, Zang YF. 2008. An improved approach to detection of amplitude of low-frequency fluctuation (ALFF) for resting-state fMRI: fractional ALFF. *J Neurosci Methods* 172:137–141.

Address correspondence to:

Jieun Kim
 Department of Radiology
 MGH/MIT/HMS Athinoula A. Martinos Center
 for Biomedical Imaging
 Massachusetts General Hospital
 #2301, 149 13th Street
 Charlestown, MA 02129

E-mail: seesaw@nmr.mgh.harvard.edu